Optimization of the level and range of working temperature of the PCM in the gypsum-microencapsulated PCM thermal energy storage unit for summer conditions in Central Poland

IOP Conf. Series: Materials Science and Engineering **251** (2017) 012117 doi:10.1088/1757-899X/251/1/012117

Optimization of the level and range of working temperature of the PCM in the gypsum-microencapsulated PCM thermal energy storage unit for summer conditions in Central Poland

P Łapka and M Jaworski
Institute of Heat Engineering, Warsaw University of Technology, 21/25 Nowowiejska St, 00-665 Warsaw, Poland

E-mail: plapka@itc.pw.edu.pl

Abstract. In this paper thermal energy storage (TES) unit in a form of a ceiling panel made of gypsum-microencapsulated PCM composite with internal U-shaped channels was considered and optimal characteristics of the microencapsulated PCM were determined. This panel may be easily incorporated into, e.g., an office or residential ventilation system in order to reduce daily variations of air temperature during the summer without additional costs related to the consumption of energy for preparing air parameters to the desired level. For the purpose of the analysis of heat transfer in the panel, a novel numerical simulator was developed. The numerical model consists of two coupled parts, i.e., the 1D which deals with the air flowing through the U-shaped channel and the 3D which deals with heat transfer in the body of the panel. The computational tool was validated based on the experimental study performed on the special set-up. Using this tool an optimization of parameters of the gypsum-microencapsulated PCM composite was performed in order to determine its most appropriate properties for the application under study. The analyses were performed for averaged local summer conditions in Warsaw, Poland.

1. Introduction

Night ventilation is a low-cost technique that may provide required indoor conditions in buildings during summer. The range of temperature variations in daily cycle depends, among others, on the rate of building cooling during the night, which in turn depends on the intensity of night ventilation while the amplitude of temperature oscillations depends on the thermal capacity of the building structure. Nowadays, the use of phase change materials (PCMs) incorporated in the building's envelope in order to increase its thermal inertia were proposed [1-6]. These materials absorb (and release in a subsequent phase of a cycle) a large amount of heat undergoing phase change process (melting/solidification) in a narrow range of temperature.

In order to achieve the benefits of use of PCMs in buildings many problems must be solved, e.g., modification of material properties [6-8], development of the methods of incorporation of these materials in the structure of the building [9-11] or enhancement of heat transfer rate between the air and PCM [12, 13].

The effective operation of the PCM based thermal energy storage (TES) system strongly depends on proper selection of the PCM for a given application, basically it is related to the temperature level and range of phase transition. Building integrated TES systems are of growing interest in recent years, since they provide the ability to efficient use of both renewable energy sources and natural variations

of ambient air temperature for air conditioning of internal space. In case the storage unit is combined with free cooling of building an adjustment of phase change temperature of the PCM to the range of daily variations of air temperature is crucial. The PCMs absorb (and subsequently release) a great amount of heat while they melt (solidify). If melting temperature level and range are incorrectly chosen with regard to the properties of the source of heat (coolness) to be stored the storage unit will not use the whole its thermal capacity. Determination of the optimal characteristics of the gypsum-PCM composite requires an analysis of heat transfer process during the whole cycle, i.e., during charging and discharging, with local climatic conditions included. In the paper such a study for the TES system integrated with the ventilation system [14] of the building operating during the summer in Central Poland is presented applying numerical modeling [15].

2. Ceiling panel TES

The ceiling panel under consideration, with basic dimensions, is shown in figure 1A. It is a board of 6 cm thickness, with 3meters long parallel channels of the square cross-section of 3×3 cm. The whole ceiling may consist of several repetitive elements (see figure 1A) with their number depending on the dimensions of the room. The combination of inlets and outlets can be made using special manifolds. The ambient air passes through two branches of the U-shaped channel before entering the interior of a building – figure 1B. When the air temperature is higher than upper range of thermal comfort temperature (during the day) it is cooled down flowing through the channel which absorbs a large amount heat (melting of PCM). During the night when the ambient air temperature is much lower than the lower limit of thermal comfort it is heated up flowing through the channel which releases heat (solidification of the PCM). For the purpose of the current study the cycling process of charging and discharging of the celling panel lasting for several days was analyzed.

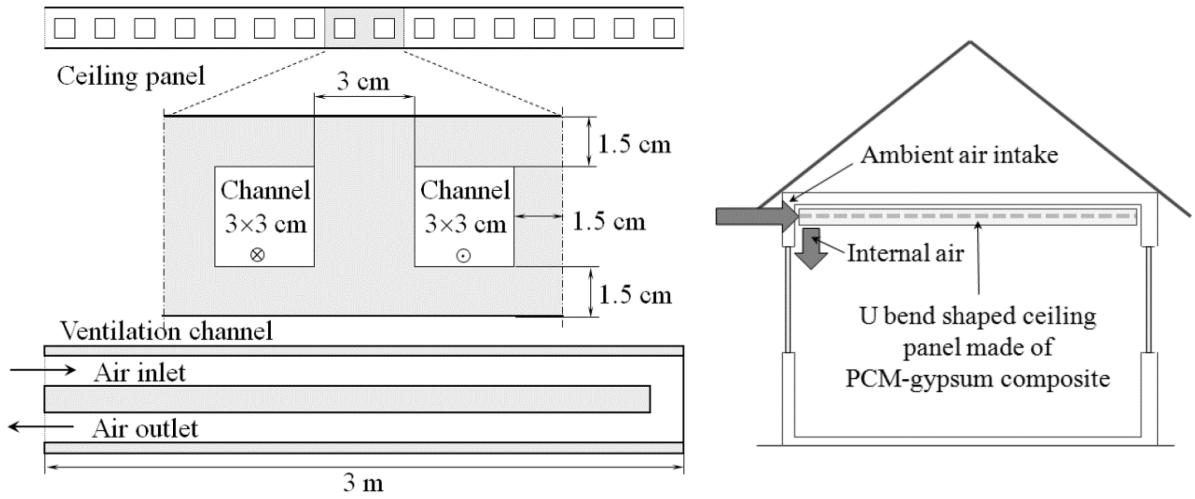

(A) (B)

Figure 1. Schematic of: A) the ceiling panel, B) the air flow direction in the celling panel.

The proposed panel was made of a composite of gypsum mortar (Knauf) and micro-encapsulated PCM (Micronal DS-5008X, BASF). The PCM content was about 27.6% wt. (30% wt. for dry components). Melting point for the PCM used in the composite equals to 22.8 °C (by DSC, Perkin-Elmer). The enthalpy vs. temperature (*h-T*) curve for this composite exhibits hysteresis between cooling and heating process and is presented in figure 2A. Thermal conductivity was also estimated with the use of mini-plate apparatus (Poensgen type) and was found to be temperature dependent according to the following relationship: $k[T(°C)] = 0.5772–0.01611T$ (W/m/ K) in the range of temperature 15-30°C [16]. Density of the composite equals to $\rho = 1000$ kg/m^3. In order to determine the optimal characteristics of the gypsum-PCM composite additional *h-T* curves were generated by

shifting the temperature range of the measured enthalpy vs. temperature curve (the base case "0") both on the left hand side (denoted by "-") and on the right hand side (dented by "+") – see figure 2B. All together ten following curves (cases) were obtained: ±1, ±2, ±3, ±4 and ±5. The range of enthalpy variations was the same for all cases.

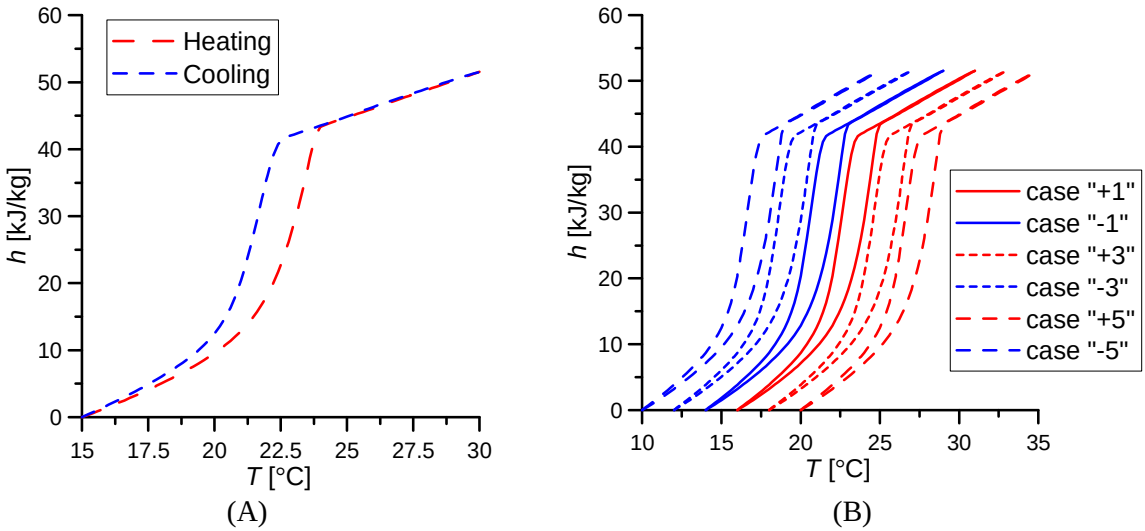

Figure 2. Enthalpy vs. temperature curves for gypsum-PCM composite: A) measured for base case "0", B) modified by shifting the temperature range by ±1, ±3 and ±5 (cases ±2 and ±4 are not shown due to legibility).

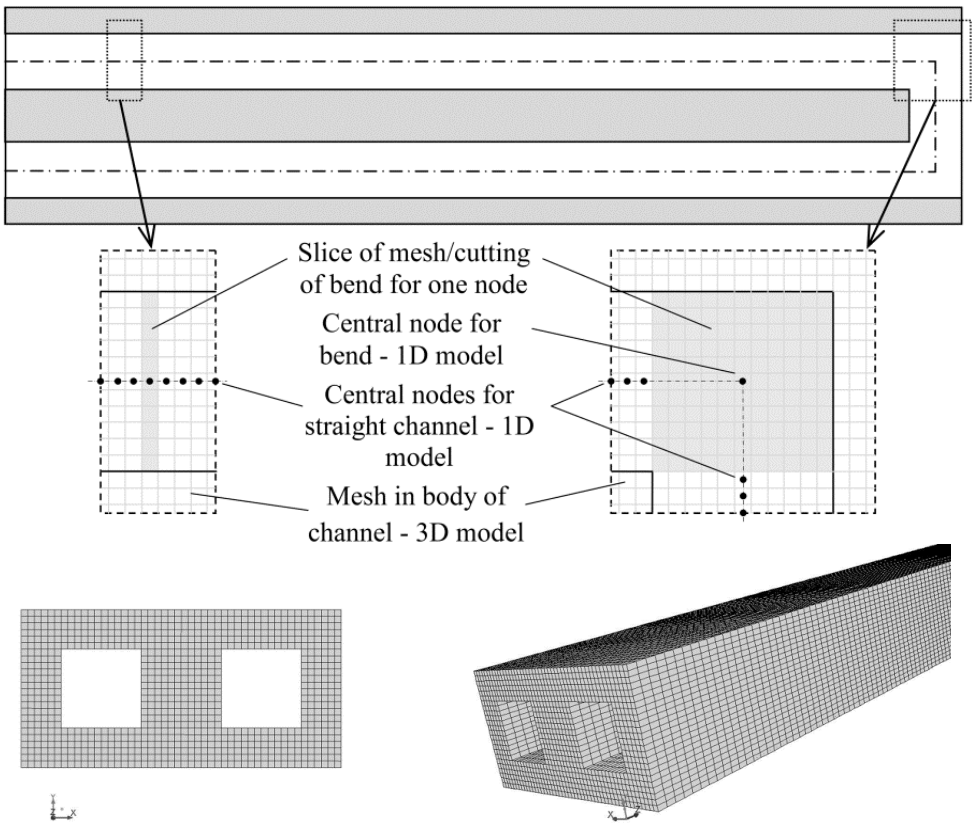

Figure 3. Schematic of the 3D/1D numerical model of the celling panel.

3. Numerical model

The novel numerical model of fluid flow and heat transfer in the celling panel under consideration was developed [15]. The model consisted of two parts: the first one – 3D – which accounts for heat transfer and phase change phenomena in the body of the panel and the second one – 1D – which deals with fluid flow and heat transfer in the air flowing through the U-shaped channel. The energy equation for 3D heat flow and phase change process in the panel was following:

$$\rho c_p\left(T,\ \text{history of } T\right)\frac{\partial T}{\partial t}=\nabla k\left(T\right)\nabla T \tag{1}$$

while the governing equation for 1D uncompressible air flow in the channel was as follows:

$$c_{p,a}\rho_a\frac{\partial T_a}{\partial t}+c_{p,a}\rho_a u\frac{\partial T_a}{\partial x}=k_a\frac{\partial^2 T_a}{\partial x^2}+\frac{P_c}{A_c}h_i\left(x\right)\left[T_a-T_{w,m}\left(t,x\right)\right] \tag{2}$$

where: A_c – cross section area of the channel, c_p – specific heat, h_i – heat transfer coefficient at internal walls of the channel, k – thermal conductivity, P_c – perimeter of the channel, t – time, T – temperature, $T_{w,m}$ – temperature of the wall of the channel averaged over the perimeter, u – air velocity, x – coordinate along the U-shaped channel, ρ – density. In equation (1) c_p depends on temperature and additionally on the history of temperature changes and was found from *h*-*T* curves (figure 2).

(A)

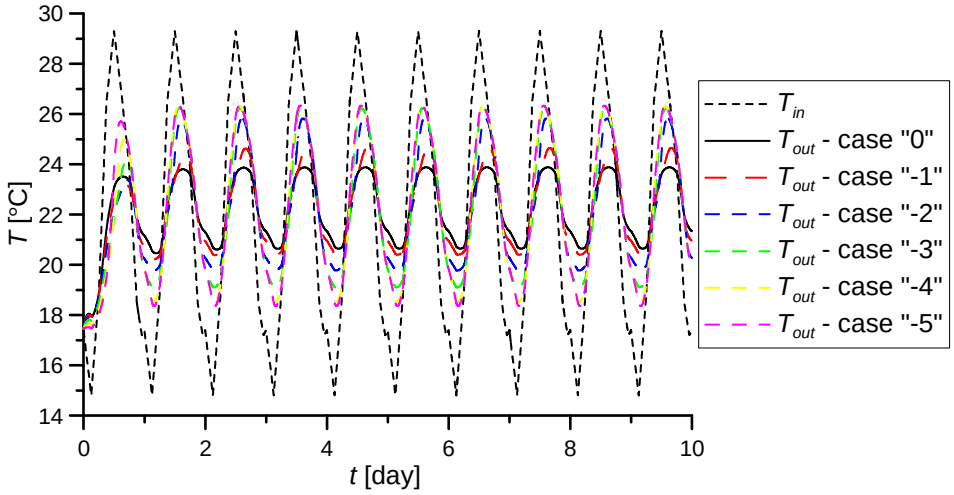

(B)

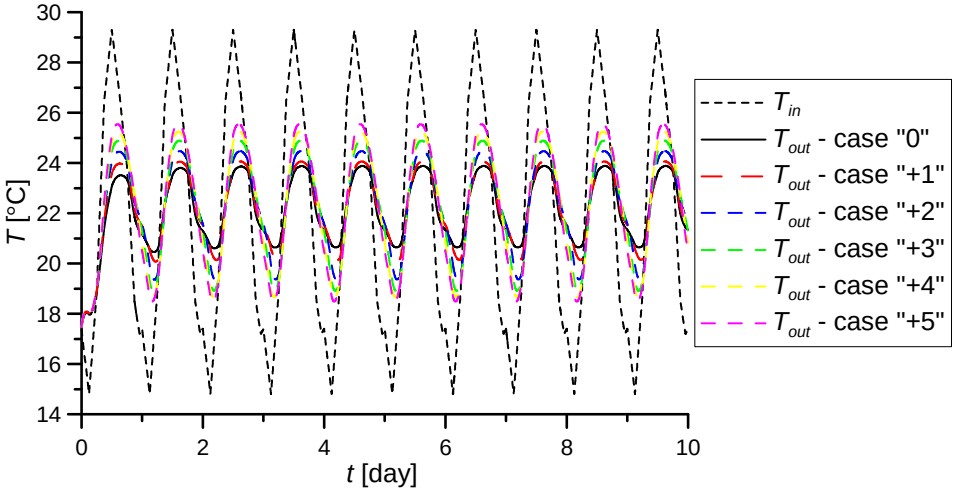

Figure 4. Inlet and exit temperature variations for inlet velocity equal to 2 m/s and for cases: A) "0", "-1", "-2", "-3", "-4" and "-5", B) "0", "+1", "+2", "+3", "+4" and "+5".

The boundary conditions for equation (1) were assumed in the following way: the top external wall was convectively cooled/heated by the surrounding air; the front, back, bottom and side external walls were adiabatic; internal walls of the channel were cooled/heated by the flowing air at temperature which varied along the flow direction x and in time t, i.e., $q_i(t,x) = h_i(x)[T_a(t,x)-T_w(t,x)]$, where: T_w – temperature of the surfaces of the U-shaped channel. The 3D model was coupled with the 1D flow model through this boundary condition. The boundary conditions for equation (2) at the inlet and exit from the channel were following: $T_a(x = 0) = T_{in}$ and $\partial T_a/\partial x(x = L) = 0$, respectively. In equation (2) the last term on the right hand side couples this 1D equation with equation (1) through the averaged wall temperature $T_{w,m}$. Uniform temperature distributions in the panel and in the flowing air were assumed as the initial conditions for equations (1) and (2), i.e., $T(t = 0) = T_{init}$.

(A)

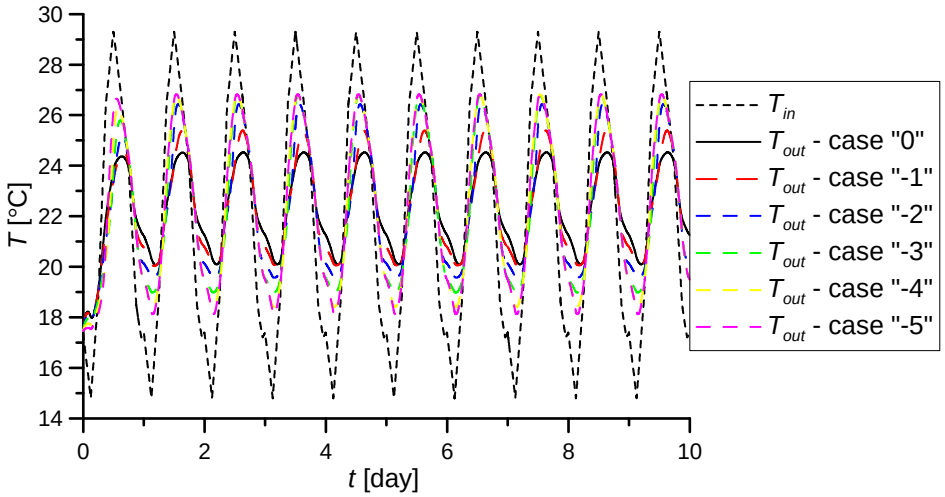

(B)

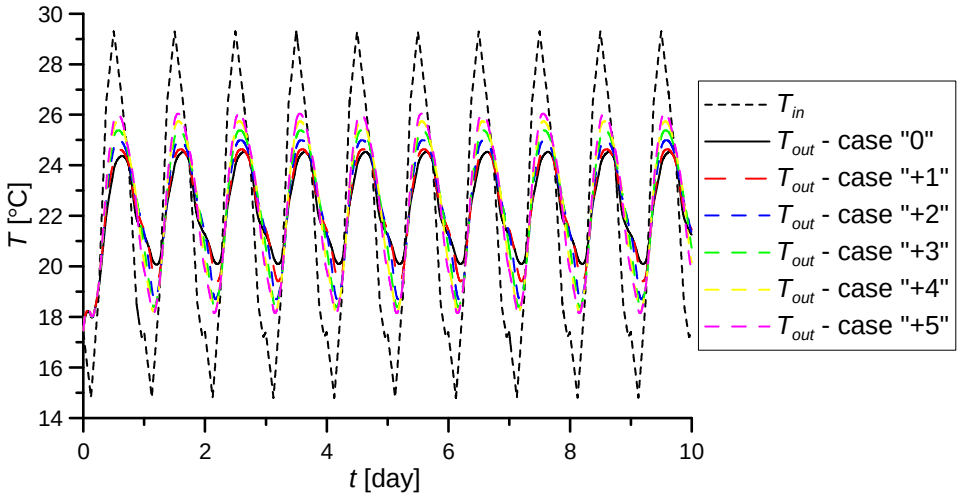

Figure 5. Inlet and exit temperature variations for inlet velocity equal to 3 m/s and for cases: A) “0”, “-1”, “-2”, “-3”, “-4” and “-5”, B) “0”, “+1”, “+2”, “+3”, “+4” and “+5”.

The general schematic of the developed 3D-1D numerical model and generated 1D and 3D meshes are presented in figure 3. For the panel cubical grid was generated while for the fluid flow line grid was created. The 1D mesh in the air was strictly connected with 3D mesh in the panel. For the straight channel the position of the central node of 1D element in the fluid coincides with the respective central nodes of 3D elements in the body of the panel. For the bend only one element in the air is used. Equations (1) and (2) were solved implicitly by applying finite volume based commercial code ANSYS Fluent 17.2 and its advanced functionalities like: User-Defined Scalar (UDS), User-Defined

Function (UDF) and User-Defined Memory (UDM). More details regarding the numerical model can be found in [15].

(A)

(B)

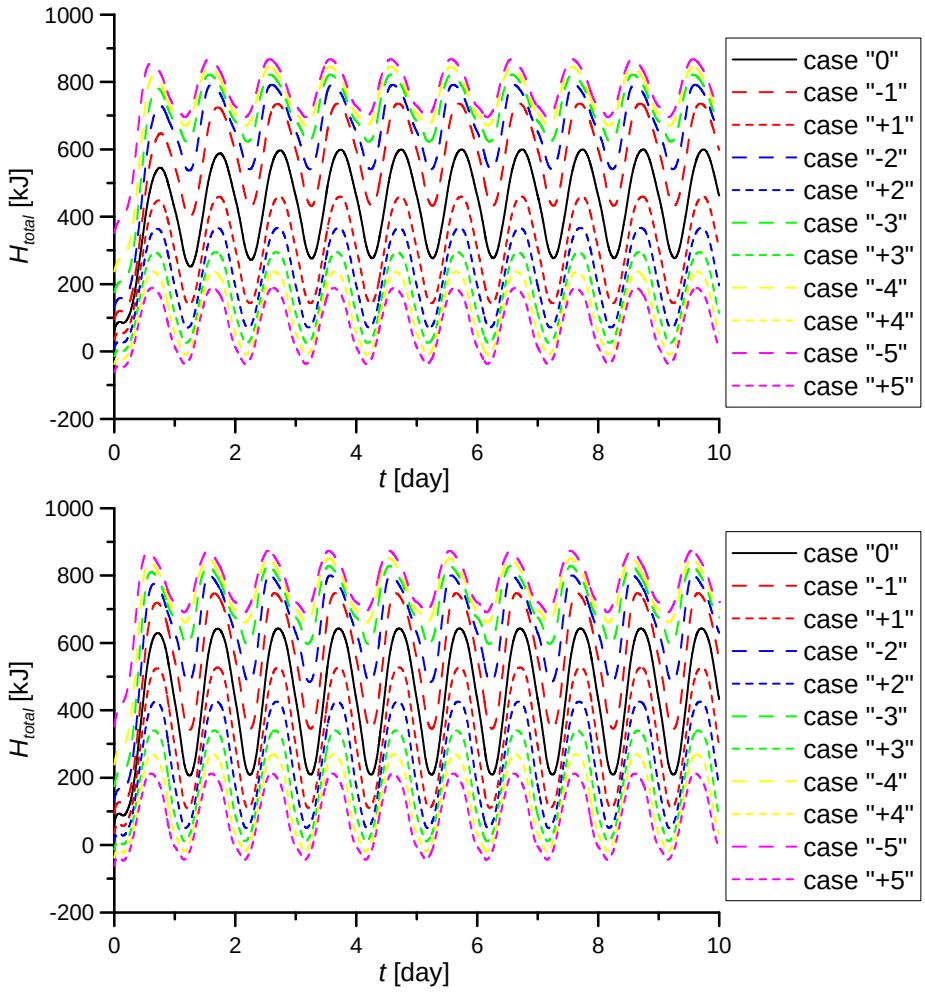

Figure 6. Total enthalpy of the panel for all considered *h-T* curves and for inlet air velocity equal to: A) 2 m/s, B) 3 m/s.

Table 1. Values of amplitude of the exit temperature of the air and values of amplitude of the total enthalpy (maximal value of absorbed heat) of the panel in the quasi-steady state for 10-th day of the cycle.

Case	"0"	"-1"	"-2"	"-3"	"-4"	"-5"	"+1"	"+2"	"+3"	"+4"	"+5"
Inlet air velocity equal to 2 m/s											
ΔT [K]	3.2	4.3	6.1	7.1	7.8	8.0	3.9	5.1	6.0	6.6	7.1
Q_{max} [kJ]	322.5	303.6	250.6	198.9	175.7	172.0	316.4	295.5	269.4	245.8	225.2
Inlet air velocity equal to 3 m/s											
ΔT [K]	4.4	5.3	6.9	7.8	8.4	8.7	5.2	6.3	7.0	7.5	7.9
Q_{max} [kJ]	434.2	402.7	316.3	231.5	191.3	182.8	416.6	375.1	328.8	288.2	255.7

4. Results of simulations

Numerical calculations were performed for two inlet velocities of the ambient air, i.e., 2 and 3 m/s and for averaged daily variations of the ambient air temperature in the region of Central Poland (Warsaw) in July. The period of 10 days (cycles) was simulated.

The variation of the inlet and outlet temperatures for *h-T* curves with different temperature range are presented in figure 4 and 5 for inlet air velocity equal to 2 and 3 m/s, respectively. The air temperature at the exit from the panel is substantially reduced for all cases. The lowest amplitudes of temperature variation were achieved for the cases "0" and "+1". This observation suggests that for the cases "0" and "+1" the PCM embedded in the body of the panel absorbed and released the largest amount of heat and therefore the TES unit operated with the highest effectiveness. The values of difference between maximum and minimum temperature observed in the cycle are presented in table 1.

In the next figure (figure 6) time variations of the total enthalpies of the panel are presented for different *h-T* curves and for two inlet velocities of the ambient air. The reference levels for specific enthalpy (h_{ref} = 0 kJ/kg) were at the temperature which corresponds to the lower limit of the *h-T* curve variation, e.g., T_{ref} = 10°C for case "-5", T_{ref} = 11°C for case "-4",… T_{ref} = 15°C for case "0",… T_{ref} = 20°C for case "+5" – see figure 2. The difference between maximum and minimum values of total enthalpy is equal to the maximum amount of heat absorbed by the panel. Its values are given in table 1.

Based on the data presented in the table 1 one can see that incorrect selection of the working temperature range of the gypsum-microencapsulated PCM composite may result in a more than two times lower thermal effectiveness of the TES unit than for the best case.

5. Conclusions

In this paper the TES unit in a form of the ceiling panel made of the gypsum-microencapsulated PCM composite with internal U-shaped channels was considered. The panel may be used as a part of the ventilation system. By applying the numerical model of the TES unit its thermal behavior for 10 day cycle and for different *h-T* curves of the gypsum-microencapsulated PCM composite were simulated. The averaged local summer conditions in Warsaw (Poland) were considered during investigations.

Applying the obtained results optimal characteristics of the gypsum-microencapsulated PCM composite were determined. It turns out that *h-T* curve with hysteresis in the range between 14 and 23°C or 15 and 24°C were optimal and for these curves the TES unit operated with the highest efficiency. Incorrect selection of the working temperature range of the gypsum-microencapsulated PCM composite leads to substantial decrease of the effectiveness of the TES unit, e.g., two times higher temperature variations at the outlet from the panel and two times lower amount of accumulated energy as compared to the case "0".

Acknowledgments

This project has received funding from the Warsaw University of Technology in the framework of statutory activity as well as from the European Union's Horizon 2020 research and innovation programme under grant agreement No 657466 (INPATH-TES).

References

[1] Raj V A A and Velraj R 2010 *Renew. Sust. Energy Rev.* **14** 2819.
[2] Kuznik F, David D, Johannes K and Roux J-J 2011 *Renew. Sust. Energy Rev.* **15** 379.
[3] Álvarez S, Cabeza L F, Ruiz-Pardo A, Castell A and Tenorio J A 2013 *Appl. Energy* **109** 514.
[4] Soares N, Costa J J, Gaspar A R and Santos P 2013 *Energ. Buildings* **59** 82.
[5] Pomianowski M, Heiselberg P and Zhang Y 2013 *Energ. Buildings* **67** 56.
[6] Veerakumar C and Sreekumar A 2016 *Int. J. Refrig.* **67** 271.
[7] Sari A and Karaipekli A. 2008 *Mater. Lett.* **62** 903.
[8] Liu C, Yuan Y, Zhang N, Cao X and Yang X 2014 *Mater. Lett.* **120** 43.

[9] Soares N, Gaspar A R, Santos P and Costa J J 2014 *Energ. Buildings* **70** 411.
[10] Navarro L, de Gracia A, Castell A and Cabeza L F 2016 *Energ. Buildings* **116** 411.
[11] Weinläder H, Klinker F and Yasin M 2016 *Energ. Buildings* **119** 93.
[12] Stritih U and Butala V 2010 *Int. J. Refrig.* **33** 1676.
[13] Wang P, Wang X, Huang Y, Li Ch, Peng Z and Yulong DY 2015 *Appl. Energ.* **142** 328.
[14] Jaworski M 2014 *Appl. Therm. Eng.* **70** 665.
[15] Jaworski M, Łapka P and Furmański P 2014 *Appl. Energ.* **113** 548.
[16] Jaworski M and Abeid S 2011 *J. Power Technol.* **91** 49.